

**The influence of fibre length, diameter and concentration on the modulus of glass fibre reinforced Polyamide 6,6.**

J. L. Thomason

University of Strathclyde, Department of Mechanical Engineering, 75 Montrose Street, Glasgow G1 1XJ, United Kingdom.

Keywords: A Polymer-matrix composites (PMCs), B Mechanical properties, E Injection moulding

**Abstract**

Results of an extensive investigation of the mechanical performance of injection moulded long glass fibre reinforced polyamide 6,6 composites are presented. The glass fibre content in these composites was varied over the range of 10-50% by weight using fibres with average diameters of 10, 14, and 17  $\mu\text{m}$ . Mechanical testing was carried out at 23°C and 150°C on dry-as-moulded and boiling water conditioned samples. The results from these composites were compared with standard extrusion compounded short glass fibre materials. The influence of fibre diameter and concentration on the residual fibre length, fibre orientation distribution and composite modulus is presented and discussed in comparison to the predictions of some of the available micromechanical models.

[James.Thomason@strath.ac.uk](mailto:James.Thomason@strath.ac.uk)

## **Introduction**

In recent years there has been strong growth in the use of long glass fibre thermoplastic composite systems in semi-structural and engineering applications. These thermoplastic matrix composite systems combine ease of processing with property advantages such as enhanced toughness and an unlimited shelf life. Furthermore, their intrinsic recyclability is rapidly being recognised as a strong driving force for their further application. Their potential for high-volume processing combined with high levels of end use property levels and associated lower manufacturing costs has spurred the current expansion of research and development activities on thermoplastic matrix composites. Glass fibre reinforced polyamides, such as nylon 6 and nylon 6,6, are excellent composite materials in terms of their high levels of mechanical performance and temperature resistance. The mechanical performance of these composites results from a combination of the fibre and matrix properties and the ability to transfer stresses across the fibre-matrix interface. Variables such as the fibre content, diameter, orientation and the interfacial strength are of prime importance to the final balance of properties exhibited by injection moulded thermoplastic composites [1-7].

Short fibre reinforced thermoplastics have been used in the automotive industry for many years and there has recently been a strong growth in the use of polyamide based materials in under-the-hood applications [8]. More recently there has been an increasing growth in the use of long fibre thermoplastic composite systems in semi-structural and engineering applications. It is interesting to note that the growth rates for polypropylene based long fibre compounds has far exceeded that of other long fibre thermoplastic systems over the last decade. This has occurred despite the fact that many of the early developments and long fibre thermoplastic products were based on polyamide resins [9-12]. It may well be that part of the background to this phenomenon lies in the excellent levels of profitability, processibility, and performance of these materials. Achieving the correct balance of these “3P’s” is critical to the success of any product in its appropriate market. Notwithstanding these facts there has been considerable discussion recently that the next major long fibre development may be in thermoplastic systems based on higher performance resins than polypropylene. Glass fibre reinforced polyamides are excellent composite materials however the mechanical properties of polyamide based composites decrease markedly upon the absorption of water and other polar fluids [13-15]. There also exist a number of well documented differences in the structure performance relationships of short

fibre reinforced polyamide and polypropylene composites and it can be expected that there will also be differences when comparing these resins reinforced with long fibres.

In this report data are presented on the mechanical performance of long fibre reinforced polyamide 6,6 which may be relevant to the above discussion. Injection moulded long fibre reinforced polyamide 6,6 samples have been prepared with a range of glass contents (0-50% wt) and two sizing chemistries for polyamide reinforcement. These long fibre compounds have been produced with glass fibres having average fibre diameters of 10, 14, and 17  $\mu\text{m}$ . Mechanical performance has been determined for both the “dry as moulded” state and after hydrolytic and temperature conditioning and compared with reference short fibre composites based on 10  $\mu\text{m}$  diameter fibre in the same resin system. The effect of process conditions on the control of the pellet fibre content observed during the long fibre pellet production process is discussed. Data on the influence of the above variables on the residual fibre length and fibre orientation distribution in the moulded composites and the composite modulus under different environmental conditions are presented and discussed. The results on composite strength and impact performance will be published in a later paper.

## **Experimental**

The glass samples used for the production of the long glass fibre pellets were continuous Advantex<sup>®</sup> glass (boron free E-glass) Type 30<sup>®</sup> packages produced on a single production bushing. The glass was coated with sizing formulation R43S, which is a polyamide compatible sizing optimized for continuous glass products. Samples (LF10, LF14 and LF17) were produced with nominal fibre diameters of 10, 14 and 17  $\mu\text{m}$  and linear density (tex) of 1200, 2400, and 3500 g/km as shown in Tables 1 and 2. A reference short fibre compound (SF10) was produced using DS1123 a nominal 10  $\mu\text{m}$  fibre diameter chopped glass product coated with polyamide sizing optimized for chopped glass production. The polyamide 6,6 (PA6,6) used for composite production was DuPont Zytel 101. Reference samples of the unreinforced resin were also included. Given that the matrix in the fibre reinforced materials experiences an extra heat cycle, reference resin samples were moulded from resin which had been run one time through the extruder with the same temperature profile as applied during the composite pellet production step.

Long fibre reinforced pellets were produced using a standard pultrusion type process where the continuous glass was fed into an impregnation unit consisting of a heated oblong box containing a number of spreader bars and a circular exit die of fixed diameter. The impregnation unit was attached to, and fed by, a single screw extruder which delivered polymer melt to the unit at a rate appropriate to the pulling speed of the glass (30 m/min) and the desired final glass:resin ratio of the pellets. The temperature of the molten resin was maintained between 300-310°C in the impregnation unit. After exiting the die the resin impregnated glass was cooled in a water bath before passing through a pulling and chopping operation. Nominal pellet chop length was 12.5 mm. For the short fibre compound, the chopped glass bundles and pre-dried PA6,6 pellets were dry blended by weight to the appropriate glass content and compounded on a single screw extruder (2.5 in., 3.75:1, 24:1 L/D screw). Set point temperatures were 288-293°C for compounding. The compounds were moulded into test bars on a 200-ton Cincinnati Milacron moulding machine. Set point temperatures were 293-299°C for moulding, at a mould temperature of 93°C.

Tensile properties were measured in accordance with the procedures in ASTM D-638, using ASTM Type I specimens at a crosshead rate of 5 mm/min (0.2 in./min) and an extensometer gauge length of 50 mm (2 in.). Tensile properties were measured “dry as moulded” (DaM) at 23°C and 150°C and at 23°C after 24 h boiling water conditioning. DaM flexural properties were measured only at 23°C in accordance with the procedures in ASTM D-790, at a crosshead rate of 2.5 mm/min (0.1 in./min) and a span width of 50 mm (2 in.). Unless otherwise stated, all mechanical property testing was performed at 23°C and at a relative humidity of 50%. Fibre length and diameters were determined by image analysis and optical microscopy on fibre samples removed from the moulded bars after high temperature ashing. Diameter was measured on 750 fibres and lengths on between 3,000 and 10,000 samples per composite sample. Measurement of fibre orientation was carried out on cross sections of moulded tensile bars cut perpendicular to the flow direction. The sections were polished and a series of optical micrographs was taken systematically across the thickness of the bar. The orientation of any fibre can be determined from its elliptical profile using the equation [16,17]

$$\cos(\phi) = W/L = 4A/\pi L^2 \quad (1)$$

where  $\phi$  is the angle the fibre axis makes with the flow direction,  $W$  is the minor axis of the ellipse which should also represent the fibre diameter,  $L$  is the ellipse major axis, and  $A$  is the area of the ellipse. Either of possibilities in equation 1 may be used, however it has been shown [17] that the greatest experimental error comes from the measurement of  $W$  and that the area method produces values with a lower degree of uncertainty. The Hermans orientation parameter ( $\eta_o$ ) can be calculated from this data using

$$\eta_o = \langle \cos^2(\phi) \rangle \quad (2)$$

where the average value of  $\langle \cos^2 \phi \rangle$  is approximated by

$$\langle \cos^2(\phi) \rangle = \frac{\sum_i [ N(\phi_i) \cos^2(\phi_i) ]}{\sum_i [ N(\phi_i) ]} \quad (3)$$

The values of  $N(\phi_i)$  must first be adjusted [18] by dividing by  $\cos(\phi_i)$  due to the lower probability of the section crossing fibres with higher values of  $\phi$ . Similarly the average fibre orientation factor ( $\eta_{oK}$ ) used in the Cox-Krenchel theory for composite modulus [19,20] can be calculated using  $\eta_{oK} = \langle \cos^4(\phi) \rangle$ .

## Results

The fibre diameter distributions of the different glass fibre samples used in this study are shown in Figure 1 and the average diameter and 95% confidence level of those averages are given in Table 1. In general it can be seen that the measured values are acceptably close to the nominal values and there is only a small amount of overlap between the adjacent distributions. The glass fibre contents of the various long fibre pellets produced for this study are shown in Table 2. From the impregnation die geometry and assuming that the material exits the impregnation die with the same circular cross section as the die exit an expected glass fibre weight content can be calculated from the following equation

$$W_f = \frac{\rho_f A_f}{\rho_f A_f + \rho_m (A_x - A_f)} \quad (4)$$

where  $\rho_f$ ,  $\rho_m$  are the fibre and resin density (at the impregnation temperature)  $A_f$  is the total fibre cross sectional area and  $A_x$  is the exit die hole area. This formula can be rearranged to give

$$W_f = \left[ 1 + \rho_m \left( \frac{A_x}{0.001T} - \frac{1}{\rho_f} \right) \right]^{-1} \quad (5)$$

where T is the glass tex (g/km),  $A_x$  is in  $\text{mm}^2$ , and densities are in g/cc. The measured values of fibre content from Table 2 are plotted against expected values calculated using equation 5 in Figure 2. An interesting trend can be observed in Figure 2 regarding the measured fibre contents. Following the lines of fixed tex, it can be seen that at the largest die diameter a measured value close to that calculated from equation 2 is obtained. As the die diameter is reduced, to obtain higher fibre contents, it can be seen that the measured fibre contents deviate to the low side. The trends of the lines in Figure 2 indicate that it becomes increasingly difficult to obtain higher fibre contents with a fixed tex by reducing the die diameter. Higher fibre contents are apparently more easily obtained by going to higher tex values of the input strands or using multiple low tex input.

The results for the weight average residual fibre length in the moulded composites are presented in Figure 3. Error bars indicate the 95% confidence limits on the averages. It is clear that 'long fibre' (LF) compounds deliver significantly longer fibres to the moulded composite in comparison to the extruded short fibre (SF) compound. The length advantage obtained with an LF process which has been well documented in polypropylene based compounds is therefore also obtained in PA6,6 materials. The relative advantage of LF/SF in Figure 3 is in the range of 1.5-3 depending on which diameter of LF is taken. This can be considered as a somewhat lower ratio than that observed in polypropylene (PP) based LF and SF materials [21]. Furthermore, the absolute values for average fibre length are significantly less than have been found with PP based LF materials. The fact that changing from PP to PA6,6 resin at the same glass content leads to shorter residual fibre lengths in the final composites is also well known from investigations of SF composites [6,13,14,21]. It is also clear that there exist significant trends for fibre length versus fibre content in Figure 3. The residual fibre length decreases strongly with increasing fibre content. As indicated in Figure 3 the data are reasonably well fit by a linear relationship with the slope of the line for the LF compounds being considerably greater than that observed for SF PA6,6 based compounds [13].

The data for Young's modulus of the moulded composites obtained from both the tensile testing and the flexural testing are shown in Figure 4. The composite modulus increases with fibre content with a somewhat increasing effect at higher glass content. In fact composite modulus scales linearly with fibre volume fraction as reviewed later in the discussion section. It is interesting to note that all data points appear to fall on a single trend line indicating that the fibre diameter in the long fibre compounds has no significant effect on composite modulus. Moreover, the data point for the short fibre reference also falls on this same trend line further indicating that fibre length does not appear to have a significant effect on Young's modulus in these materials. It can be also seen the trends for tensile modulus and flexural modulus are almost identical. However a direct comparison of the Young's modulus obtained from the two test methods shown in Figure 5 shows that there is a systematic deviation from a direct one to one relationship. The least squares fitted regression line shown in Figure 5 indicates that the value obtained from flexural testing is 7% lower than that obtained by tensile testing.

The results of the boiling water conditioning on the Young's modulus of these samples are summarised in Figures 6 and 7. These figures clearly illustrates the plasticizing effect of water on PA6,6 and its composites. The water absorption leads to a reduction of the glass transition temperature ( $T_g$ ) of the PA6,6 from the DaM value of 80 °C to below the testing temperature of 23 °C, with an equilibrium moisture content at 100 °C of approximately 16% wt. the  $T_g$  of the matrix can be estimated at approximately -20°C [22]. The resin modulus is reduced by 80% and this has a significant effect on the modulus of the composites with a reduction of 40-50% observed over the range of glass fibre content in this study with higher fibre content samples exhibiting a greater level of modulus retention. Despite this significant reduction in performance, a linear relationship between modulus and fibre volume fraction is still evident in the conditioned samples. Furthermore, there is no evidence of a significant difference in the modulus of composite with different fibre diameters after this short term conditioning. However, it does appear that the short fibre SF10 reference sample has suffered a somewhat greater loss, significant at the 95% confidence level, in modulus due to the boiling water conditioning. The results of the tensile testing at 150°C are presented in Figure 8. The trends observed are almost identical to those discussed in the above on the influence of boiling water conditioning of tensile performance. With the test temperature of 150 °C well above the glass  $T_g$  of the amorphous sections of the

polymer matrix molecules of 50 °C the modulus of the matrix is reduced by approximately 84% with a consequent 40-60% reduction in the composite modulus depending on the fibre content. Once again the SF samples appear to have suffered a greater loss in performance at 150 °C compared to the LF samples of equal fibre diameter and content. The results of the optical analysis of fibre orientation parameter following equations 1-3 are presented as  $\eta_o = \langle \cos^2(\phi) \rangle$  in Figure 9. The relatively high level of fibre orientation (average  $\eta_o = 0.80$ ) is typical of injection moulded composites. There are no significant trends observed in the results of the average fibre orientation factor relative to the average fibre concentration or the average fibre diameter.

## Discussion

It has been well documented recently that for improved mechanical performance of discontinuous fibre reinforced thermoplastics, in general, longer residual fibre length is better [7,9,12,16,21]. However, it is clear from the results in Figure 3 that, when dealing with the injection moulding process, the residual fibre length is not a property that can be directly controlled in the final composite part. The fibre length in the moulded composite is a property which is influenced by the input fibre length, the composite fibre content and the diameter of fibres employed. This may well be due to the fact that decreased average fibre diameter at equal fibre loading, or increased fibre content at equal fibre diameter, leads to a decreased average fibre-fibre spacing and consequently an increased probability of fibre-fibre and fibre-machine interaction with resultant fibre damage and breakage. This decreased fibre-fibre spacing also leads to an increased apparent melt viscosity resulting in higher bending forces on the fibres during moulding. It is interesting to note that, when the results in Figure 3 are examined in terms of residual fibre aspect ratio (length/diameter), the data for the various LF compounds collapse onto a single line. In the commercially important fibre content range of 30-40% the LF compounds deliver a residual fibre aspect ratio after moulding approximately 50% higher compared to the SF compounds.

The main factors affecting the Young's modulus of injection moulded test bars are the fibre content, stiffness, and orientation, and the matrix stiffness [4,7,13,21,23,24]. To a lesser extent the aspect ratio, in the normal range found in these samples, also plays a role. In order to be able to accurately predict composite properties it

is clearly important to have robust micromechanical models and accurate values for these input parameters. Despite the fact that many of the underlying structure-performance relationships for composite materials scale with the fibre volume fraction, most practical mouldings are mixed according to weight fractions. The fibre weight fraction ( $W_f$ ) in polymer composites is commonly determined by determining the residual fibre weight after ashing the sample at high temperature (as described in the experimental details of this paper) and the fibre volume fraction ( $V_f$ ) is then calculated from fibre weight fraction using the equation

$$V_f = \left[ 1 + \frac{\rho_f}{\rho_m} \frac{1 - W_f}{W_f} \right]^{-1} \quad (6)$$

which requires both the fibre  $\rho_f$  and matrix density  $\rho_m$  as input parameters. It is common practice to use the resin density as the matrix density (for DaM PA6,6 = 1.130 g/cc). For an appropriate analysis of the fibre contribution to the composite modulus it is necessary to have an appropriate value for the fibre volume fraction available. Equation 6 is adequate to estimate the volume fraction of the DaM samples in this study, however certain modifications are necessary in the case of the two types of conditioning used prior to mechanical testing.

It has recently been shown how the fibre volume fraction calculated from the fibre weight fraction of a dry sample must be adjusted to take into account the change in sample dimension and weight due to any conditioning that may have been applied to the samples [13-15]. In this case the adjustment for properties measured at high temperature must account for the change in volume of the fibre and matrix due to their thermal expansion. For moisture conditioned samples, tested at room temperature, it can be assumed that the fibre is unchanged; however the weight and density of the matrix must be adjusted for the absorption of water. Using volumetric thermal expansion coefficients for the glass of  $18 \times 10^{-6} \text{ C}^{-1}$  and for the resin of  $360 \times 10^{-6} \text{ C}^{-1}$ , and a PA6,6 equilibrium moisture content at 100 °C of 16 % w/w an adjusted fibre volume fraction can be calculated for each sample. These data for fibre volume fraction calculated using equation 6 for all three conditions are shown in Figure 10 as a function of the original composite fibre weight fraction. For the samples tested at 150 °C the change is an approximate 4.3% reduction in fibre volume fraction while for the

boiling water conditioned samples the reduction is much greater in the 11-13% range. These differences have a significant effect on the analysis of the fibre contribution to composite properties.

The fibre orientation and aspect ratio in injection moulded composites are complex quantities which, unfortunately, are not independent variables. It is well known that injection moulded composites often exhibit a complex distribution of fibre orientations due to the interactions between melt properties and moulding conditions. As the melt fills the mould there is fountain flow which initially orients the fibres and polymer molecular chains perpendicular to the main flow direction. Fountain flow causes the melt to be deposited on the mould wall with the alignment direction parallel to the mould fill direction. Here it solidifies rapidly and this alignment is retained in the solid article. Further behind the melt front, shear flow dominates and produces fairly uniform levels of fibre alignment. In the very centre of the melt the rate of shear is low and the transverse fibre alignment present at the gate is retained. These general features are apparent in studies of fibre orientation distribution found in the [4,6,16,17] literature and lead generally to the formation of a multi-layered structure referred to as skin-core for a three layer structure or skin-shell-core for more complex structure. The average fibre orientation ( $\eta_o$ ) and in some cases the fibre content of these layers has been shown to vary from layer to layer and in particular to be dependent on the material and process parameters.

Figure 11 shows the values of  $\eta_o = \langle \cos^2(\phi) \rangle$  obtained from a series of micrographs taken across the thickness of three of the injection moulded tensile bars from this work. All samples exhibit an orientation dependence on position through the thickness which is associated with a five layer skin-shell-core structure [4]. A thin outer skin layer shows a near random in-plane fibre orientation ( $\eta_o = 0.5$ ) and a thick inner core with a similar level of near random fibre orientation. In between this inner core and the outer skin layer there is also a relatively thick shell layer where the fibres are strongly oriented in the melt flow direction ( $\eta_o = 0.75-0.9$ ). Akay and Barkley [4] observed a very similar microstructure in their study of injection moulded long fibre thermoplastics. They observed a skin layer which had a random fibre orientation and a fairly constant thickness of 5% of the sample thickness and core and shell layer thicknesses which were dependent on moulding conditions. The data in Figure 11 also indicate a skin layer of approximately 1/24 (or 4%) of the sample thickness. Although the existence of these layered structures in injection moulded composites is well known their effect on the relative tensile and flexural performance of such composites has not been greatly

explored to date. Given the fact that the tensile performance should give an equally weighted average over the thickness of the specimen whereas the flexural test will generate data which is strongly influence by the outer layers of the sample this may well be the source of the systematic differences observed in tensile and flexural modulus shown in Figure 5. Given that the flexural modulus is systematically lower than the tensile modulus the implication is that one of the outer layers has a significantly lower average modulus value. This could be due to local (low) variation of the fibre content, local (lower) levels of average fibre length, a lower level of average fibre orientation in the loading direction, or more likely a combination of these factors. Unfortunately further exploration of these possibilities required a level of characterisation which was beyond the scope of this work.

The common micromechanics approaches to analyzing data for the composite tensile modulus using simple “rule-of-mixtures” techniques have previously been discussed in some detail [6,13,15,21,23,24]. The robustness of any particular model is related to its ability to reasonably predict composite properties over the widest range of input parameters and conditions without the necessity of introducing changes to the model. The range of fibre lengths, diameters and concentrations combined with the changes in matrix properties brought about by the different conditioning procedures make this data set a useful one for probing the robustness of the various models available for predicting composite modulus. One approach is to calculate the composite modulus  $E_c$  using the equation.

$$E_c = \eta_0 E_1 + (1 - \eta_0) E_2 \quad (7)$$

where  $E_1$  and  $E_2$  are obtained from the Halpin-Tsai equations [25] for the modulus of a unidirectionally reinforced laminate.

$$E_j = E_m \left[ \frac{1 + \xi_j \eta_j V_f}{1 - \eta_j V_f} \right] \quad \eta_j = \frac{\left( \frac{E_f}{E_m} \right)^{-1}}{\left( \frac{E_f}{E_m} \right)^{-1} + \xi_j} \quad j = 1, 2 \quad \xi_1 = \frac{2L}{D} \quad \xi_2 = 2 \quad (8)$$

where  $E_f$ ,  $E_m$ ,  $V_f$ , are the fibre and matrix stiffness and the fibre volume fraction, and  $L/D$  is the fibre length to diameter ratio. It has previously shown that this method produces very similar values of  $\eta_0$  to those obtained from the Cox analysis for injection moulded short glass fibre reinforced PA6,6. However this approach was

found [13,15] to produce modulus values with poor correlation to experiment when used to analyze data for these materials after hydrolysis conditioning at elevated temperature. Figure 12 compares modulus values for all three testing conditions obtained using equations 7 and 8 and compared against the experimentally obtained moduli. It can be seen that this method does give a good correlation for the DaM series of samples, but the predictions for the conditioned samples are very low compared to the experimental values. It was found that only by use of physically unreal input values such as  $\eta_o > 1$  or  $E_f > 150$  GPa could a good correlation be obtained. It can therefore be concluded that although the Halpin-Tsai approach appears to work acceptable for DaM samples, it is definitely not suited to a situation where the testing occurs above the glass transition temperature of the resin and the tensile modulus of the resin is low.

Another approach to modeling composite modulus is to use the following modified rule of mixtures equation

$$E_c = \eta_{oK} \eta_l V_f E_f + (1 - V_f) E_m \quad (9)$$

where  $\eta_l$  and  $\eta_{oK}$  are efficiency factors related to fibre length and orientation as introduced by Cox and Krenchel [19-21,23,24]. If the fibre length distribution is known then the modifying factor  $\eta_l$  can be calculated using the Cox shear lag method [19]. Combining these values with the experimental values for fibre volume fraction, average orientation parameter and matrix modulus results in the composite modulus values shown in Figure 13. Linear regression analysis indicates a straight line correlation of all three sets of data with a high confidence limit. It can be seen that this method appears to somewhat underestimate the modulus of the DaM series of samples. When considering the data for all three conditions in Figure 13 the spread is much narrower and is reasonably closely correlated with a line of slope=1 ( $Y=0.95X$ ,  $R^2=0.95$  for the full data set). The deviations from a line of slope=1 are within the likely total level of experimental error involved in the various input parameters required and in this case physically unrealistic alterations to the model are not required to obtain better correlation. This indicates that this model is more robust in its ability to handle quite extreme variations in the input parameters and still give reasonable predictions of the experimentally determined moduli.

More recently Fu and Lauke [26,27] have published a model for prediction of the elastic modulus of injection moulded SF polymers which contain both a fibre length distribution and fibre orientation distribution. The reader is referred to the original papers for the full details of their model. However, the basis of the model is the application of a laminate analogy where the elastic modulus of the composite is the result of integration over the contribution of model laminate plies containing fibres of any particular individual length and orientation. It is also worthy to note here that this approach uses the Cox shear-lag model for the calculation of the longitudinal  $E_{11}$  of an individual ply and the Halpin-Tsai approach for the transverse modulus  $E_{22}$  and the in-plane shear modulus  $G_{12}$ . Results for the prediction of composite modulus are compared with the experimental data in figure 14. It can be seen that this model also gives values which give an excellent linear correlation with the experimental data. It is noted that in all cases the model appears to underestimate the measured composite modulus, however the differences are also likely to be within the full range of the experimental error on the various input values. When considering the data for all three conditions in Figure 14 the spread in the data is the narrowest of the three approaches studied with a line  $Y=0.93X$ ,  $R^2=0.98$  for the full data set. Consequently this approach appears to underestimate the composite modulus slightly more than the Cox-Krenchel approach but also appears to be more robust in terms of making modulus predictions over the wide range of experimental conditions of interest with this type of composite material.

## **Conclusions**

In LFPA pellet production higher fibre contents were more easily obtained by going to higher linear density values of the input strands as opposed to reducing the die hole diameter. LFPA compounds delivered significantly longer fibres to the final moulded composite in comparison to an extruded SFPA compound. The relative length advantage of LF/SF was in the range of 1.5-3 in PA6,6 depending on average fibre diameter. The relative LF/SF residual fibre aspect ratio was found to be approximately 1.5 independent of fibre diameter. Furthermore, the absolute values for average fibre length were significantly less in LFPA than in LFPP. The average residual fibre length of all LFPA samples exhibited a strong inverse dependence on fibre content.

Fibre length and diameter over the range of this study did not have a significant effect on composite modulus. However modulus scaled linearly with fibre volume fraction. The Young's modulus determined by flexural testing gave values systematically 7% lower than those values obtained by tensile testing. It is proposed that this phenomenon is related to the complex fibre orientation layered structure in these materials. Tensile testing results at 150°C and after boiling water conditioning showed similar severe loss in stiffness and strength due to plasticisation of the PA6,6 matrix. The Halpin-Tsai approach was found unsuitable for modeling composite modulus where the testing occurred above the glass transition temperature of the matrix. Overall the Cox-Krenchel model was better for modulus prediction over all three conditions but did somewhat underestimate the DaM values. The Fu-Lauke approach proved to be the most robust of the models studied although it appeared to underestimate the experimental modulus to a slightly greater degree than the Cox-Krenchel model.

### **Acknowledgements**

The author gratefully acknowledges the support of Owens Corning and 3B Fiberglass with the preparation and testing of the materials used in this study.

## **List of Figures**

Figure 1 Fibre diameter distributions of input fibre products

Figure 2 Comparison of measured and calculated glass contents

Figure 3 Residual weight average fibre length versus fibre content

Figure 4 Youngs' modulus versus fibre content

Figure 5 Flexural versus Tensile Youngs' modulus

Figure 6 Young's modulus after 24 hour boiling water conditioning

Figure 7 Modulus retention after 24 hour boiling versus fibre content

Figure 8 Young's modulus DaM at 150 °C

Figure 9 Fibre orientation parameter from optical analysis

Figure 10 Fibre volume fraction versus weight fraction

Figure 11 Fibre orientation parameter across sample thickness

Figure 12 Comparison of Halpin-Tsai model predictions against experimental values

Figure 13 Comparison of Cox-Krenchel model predictions against experimental values

Figure 14 Comparison of Fu-Lauke model predictions against experimental values

## References

1. Sato N, Kurauchi T, Sato S, and Kamigaito O. Mechanism of fracture of short glass fibre-reinforced polyamide thermoplastic. *J. Mater. Sci.* 1984;19:1145-1152
2. Sato N, Kurauchi T, Sato S, and Kamigaito O. Reinforcing mechanism by small diameter fiber in short fiber composites. *J. Compos. Mater.* 1998;22:850-873
3. Horst JJ, and Spoomaker JL. Fatigue fracture mechanisms and fractography of short-glass fibre-reinforced polyamide 6. *J. Mater. Sci.* 1997;32:3641-3651.
4. Akay M, Barkley D. Fibre orientation and mechanical behaviour in reinforced thermoplastic injection mouldings. *J.Mater. Sci.* 1991;26:2731-42
5. Laura DM, Keskkula H, Barlow JW, Paul DR. Effect of glass fiber surface chemistry on the mechanical properties of glass fiber reinforced, rubber-thoughened nylon 6. *Polymer* 2002;43:4673-4687
6. Thomason JL. The influence of fibre properties of the performance of glass-fibre-reinforced polyamide 6,6. *Comp. Sci. Tech.* 1999;59:2315-2328.
7. Hassan A, Yahya R, Yahaya AH, Tahir ARM, Hornsby PR. Tensile, Impact and Fiber Length Properties of Injection-molded Short and Long Glass Fiber-reinforced Polyamide 6,6 Composites. *J.Reinforced Plastics and Composites* 2004;23:969-986.
8. Carlson E, Nelson K. Nylon under the hood: history of innovation. *Automotive Engineering* 1996;104:84-89.
9. Guyot H. VERTON in Long Fibres. *Plast. Mod. Elastom.* 1985;37(5):44-45.
10. Toll S, Aronsson C-G. Notched Strength of Long- and Short-Fibre Reinforced Polyamide. *Comp. Sci. Tech.* 1992;46:43-54.
11. Belbin GR, Staniland PA. Advanced Thermoplastics and their Composites. *Philosophical Transactions of the Royal Society of London. Series A, Mathematical and Physical Sciences.* 1987;322:451-464.
12. Bailey RS, Davies M, Moore DR. Processing property characteristics for long glass fibre reinforced polyamide. *Composites* 1989;20:453-460.
13. Thomason JL. Structure-property relationships in glass reinforced polyamide: 1) The effect of fibre content. *Polym.Composites* 2006;27:552-562.

14. Thomason JL. Structure-property relationships in glass reinforced polyamide: 2) The effects of average fibre diameter and diameter distribution. *Polym.Composites* 2007;27:331-343.
15. Thomason JL. Structure-property relationships in glass reinforced polyamide: 3) Effects of hydrolysis ageing on the dimensional stability and performance of short glass-fibre reinforced Polyamide 66. *Polym.Composites* 2007;27:344-354.
16. Toll S, Andersson PO. Microstructure of long- and short-fibre reinforced injection moulded polyamide. *Polym.Composites*. 1993;14:116-125.
17. Toll S, Andersson PO. Microstructural characterization of injection moulded composites using image analysis. *Composites*, 1991;22:298-306.
18. Bay RS, Tucker CL. Stereological measurement and error estimates for three-dimensional fiber orientation. *Polym. Eng. Sci.* 1992;32:240-253.
19. Cox HL. The elasticity and strength of paper and other fibrous materials. *Brit.J.Appl.Phys.* 1952;3:72-79.
20. Krenchel H. *Fibre Reinforcement*. Akademisk Forlag, Copenhagen, 1964.
21. Thomason J.L. The influence of fibre length and concentration on the properties of glass fibre reinforced polypropylene: 5) Injection moulded long and short fibre PP, *Composites Part A* 2002;33:1641-1652.
22. Starkweather HW. *Transitions and Relaxations*. Nylon Plastics Handbook, Carl Hanser Verlag, Munich 1995.
23. Thomason JL, Vlug MA. The influence of fibre length and concentration on the properties of glass fibre reinforced polypropylene: 1) Tensile and Flexural Modulus. *Composites* 1996;27A:477-484.
24. Robinson IM, Robinson J M. The influence of fibre aspect ratio on the deformation of discontinuous fibre-reinforced composites. *J. Mater. Sci.* 1994;29:4663-4677.
25. Halpin JC, Kardos JL. The Halpin-Tsai equations: A review. *Polym.Eng.Sci.* 1976;16:344-352.
26. Fu SY, Lauke B. The elastic modulus of misaligned short-fibre-reinforced polymers. *Comp. Sci. Tech.* 1998;58:389-400
27. Fu SY, Lauke B. An analytical characterization of the anisotropy of the elastic modulus of misaligned short-fibre-reinforced polymers. *Comp. Sci. Tech.* 1998;58:1961-1972.

Nominal Fibre Diameter ( $\mu\text{m}$ )	Input Tex (g/km)	Average Diameter ( $\mu\text{m}$ )	95% C.L. ( $\mu\text{m}$ ) (N=750)
10	Short Glass	9.88	0.06
10	1200	10.04	0.06
14	2400	13.97	0.09
17	2400	16.51	0.14
17	3500	17.20	0.10

**Table 1 Glass fibre tex and diameter**

Sample Code	Input Tex (g/km)	Die Exit Hole Diameter and Resultant Pellet Glass Content (% wt)			
		1.9 mm	2.3 mm	3.0 mm	4.0 mm
LF10	1200	26.7	24.6	18.5	12.2
LF10	1200x2		39.7	29.7	
LF14	2400	44.1	40.5	31.0	20.6
LF17	3500		50.8	39.3	25.9
LF17	2400	44.8		31.8	19.9

**Table 2 Composite glass contents versus production conditions**

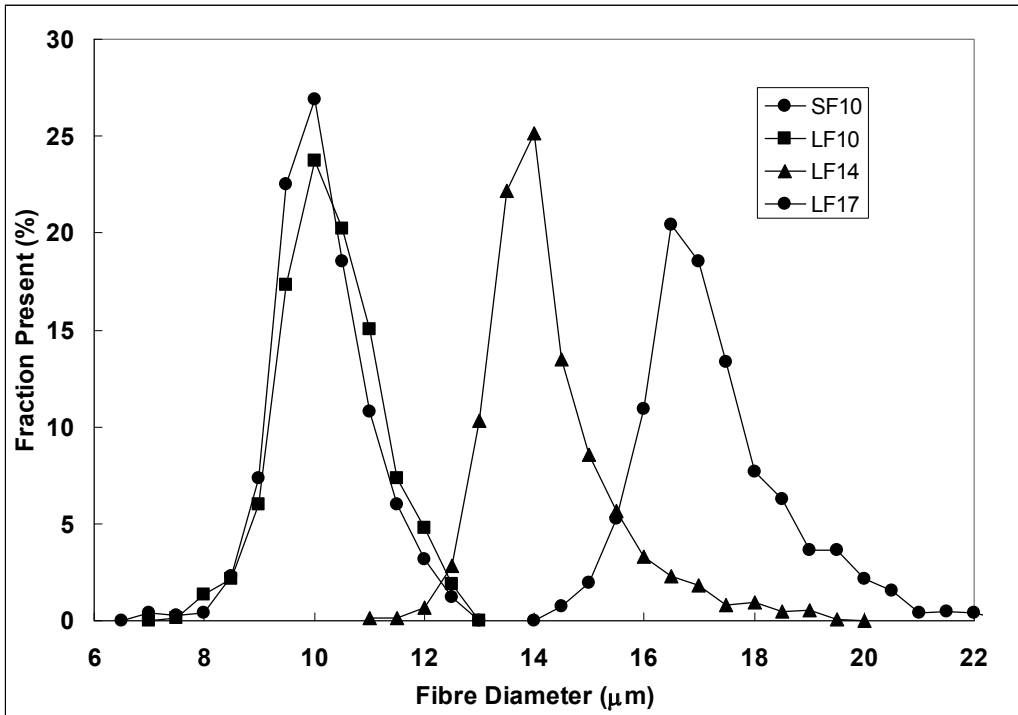


Figure 1 Fibre diameter distributions of input fibre products

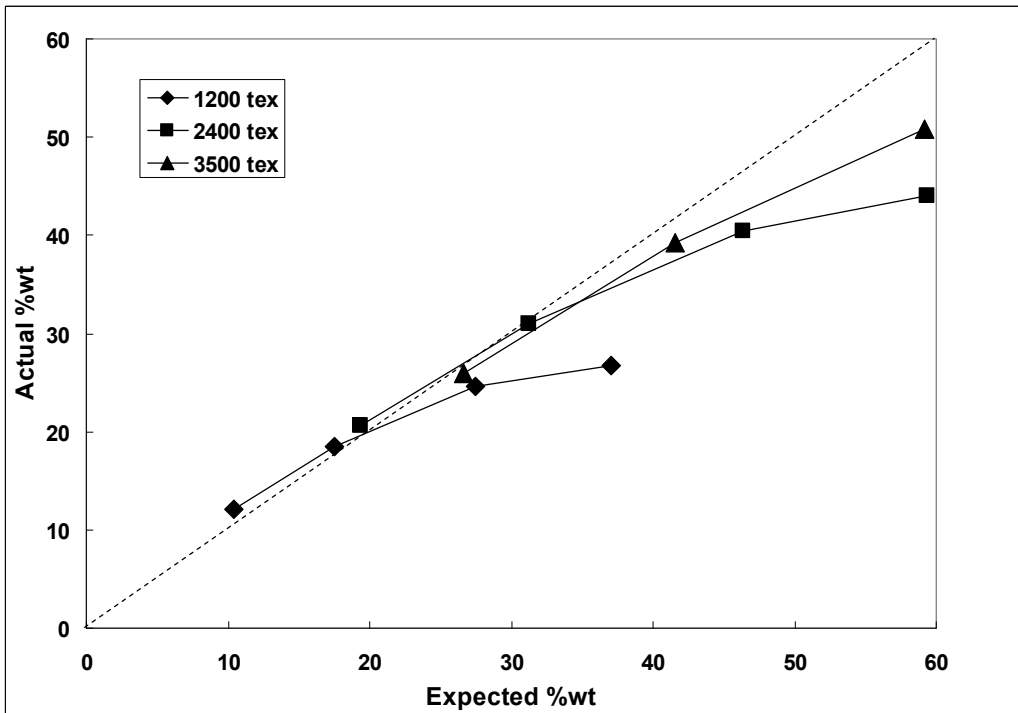


Figure 2 Comparison of measured and calculated glass contents

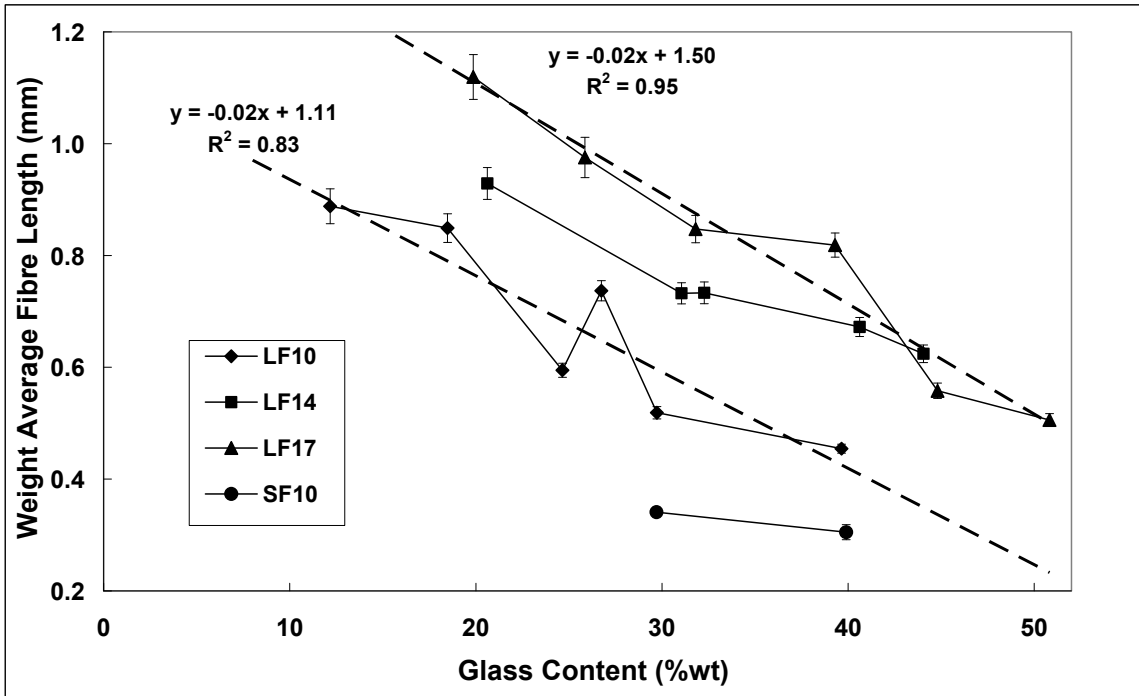


Figure 3 Residual weight average fibre length versus fibre content

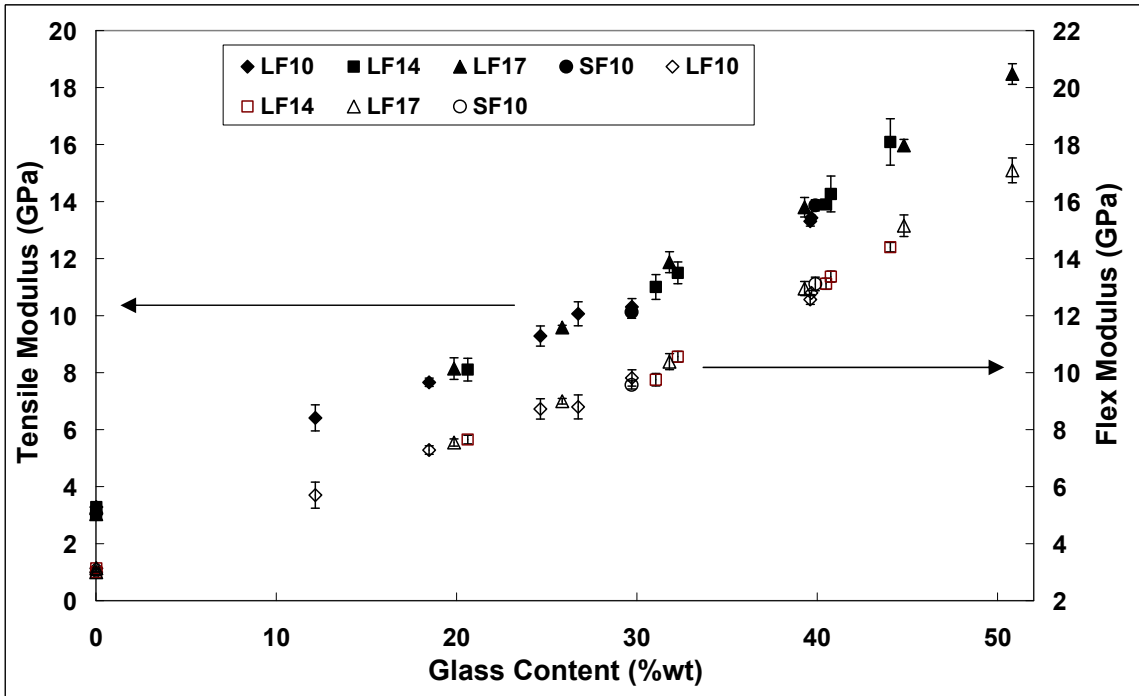


Figure 4 Youngs' modulus versus fibre content

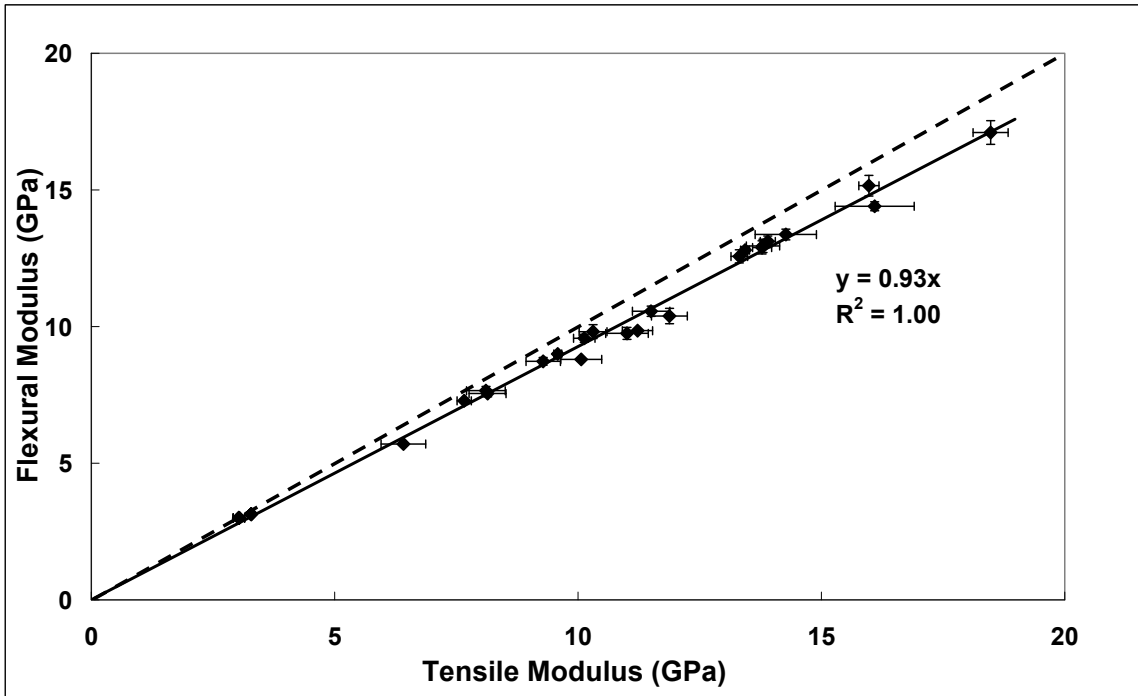


Figure 5 Flexural versus Tensile Youngs' modulus

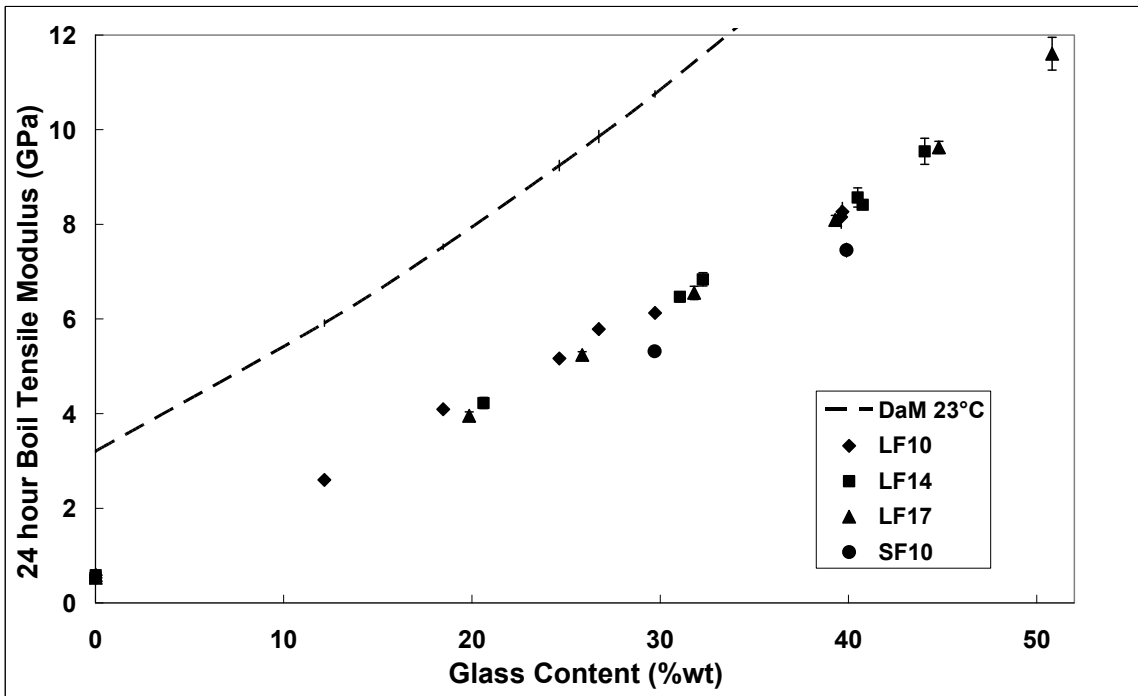


Figure 6 Young's modulus after 24 hour boiling water conditioning

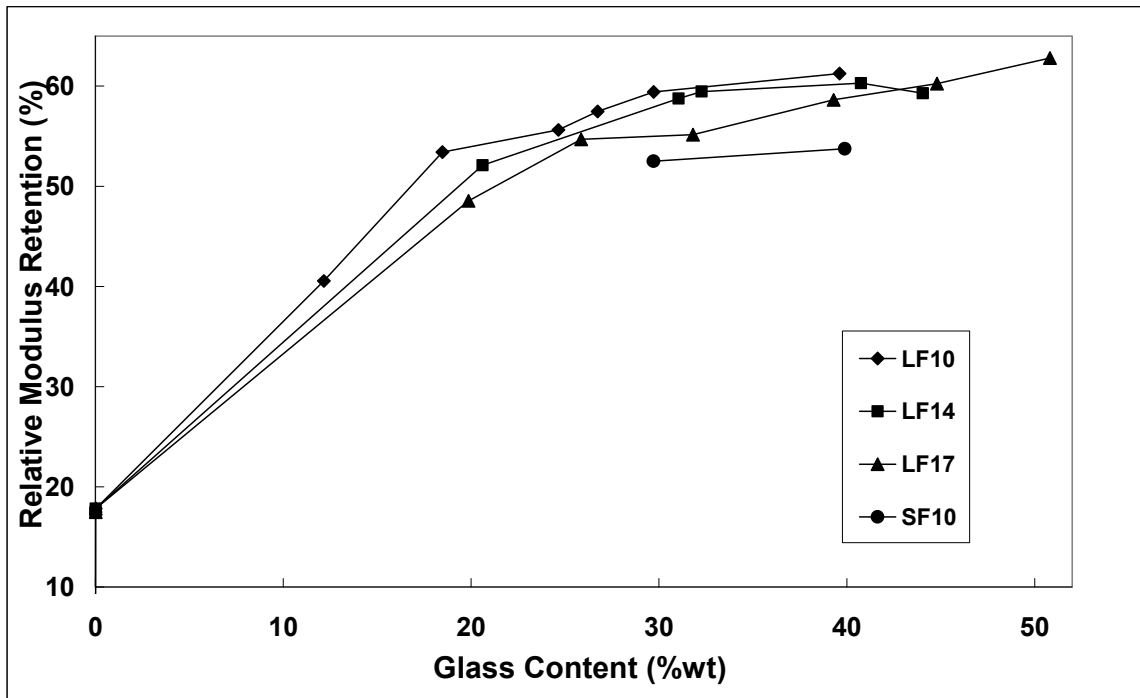


Figure 7 Modulus retention after 24 hour boiling versus fibre content

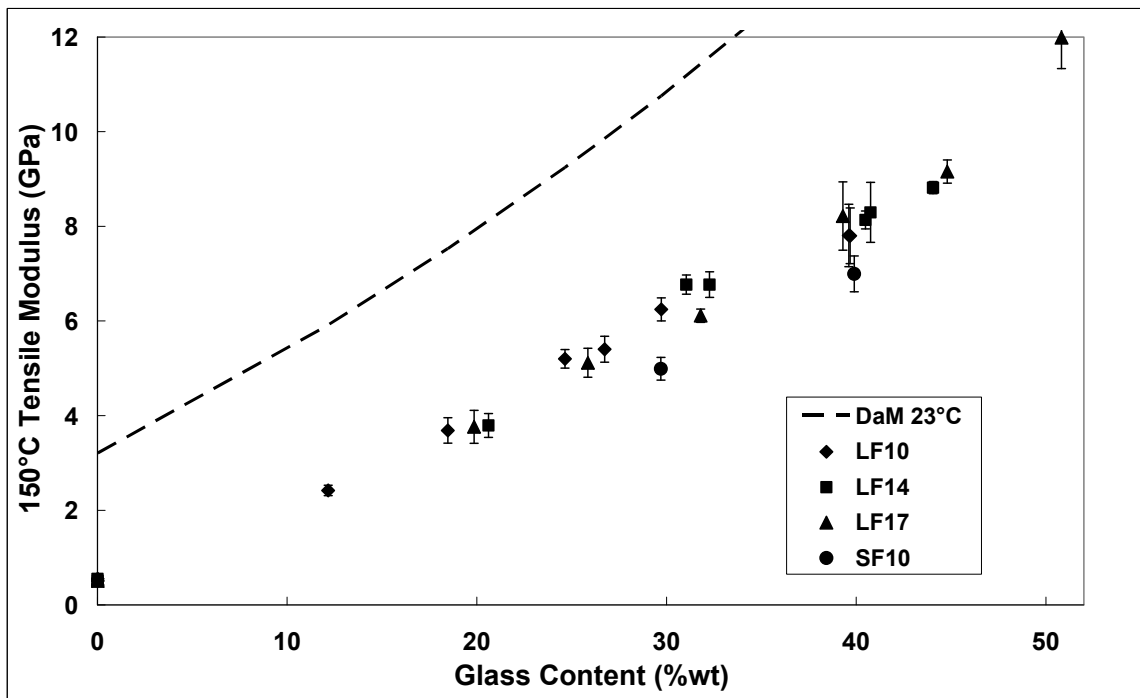


Figure 8 Young's modulus DaM at 150 °C

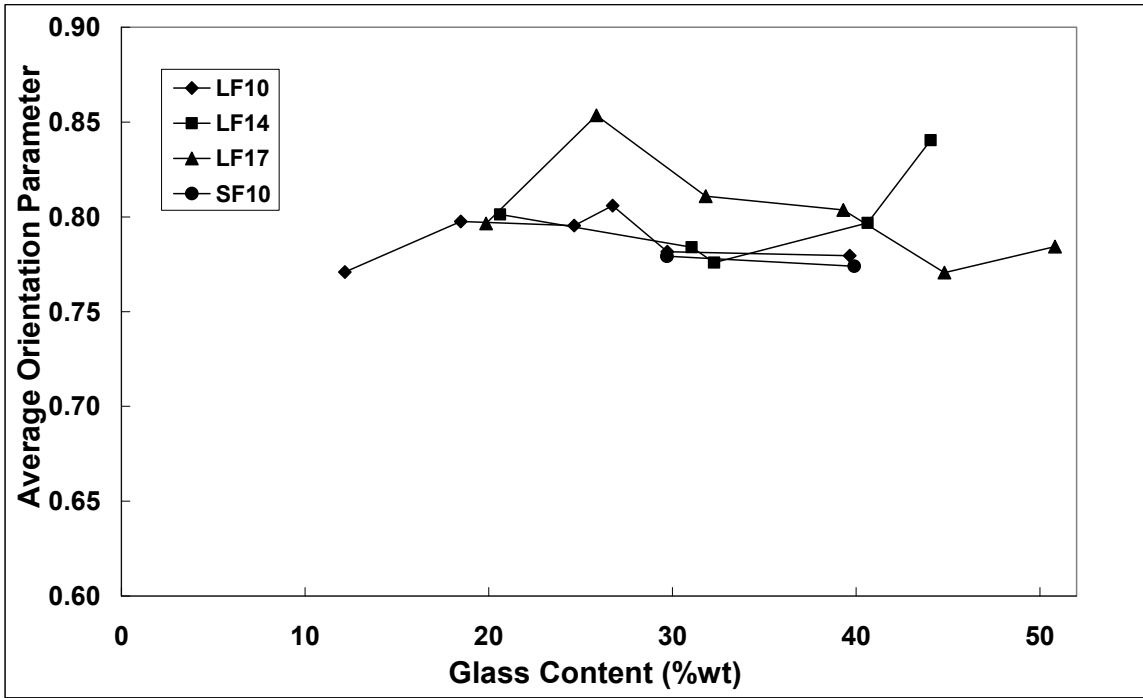


Figure 9 Fibre orientation parameter from optical analysis

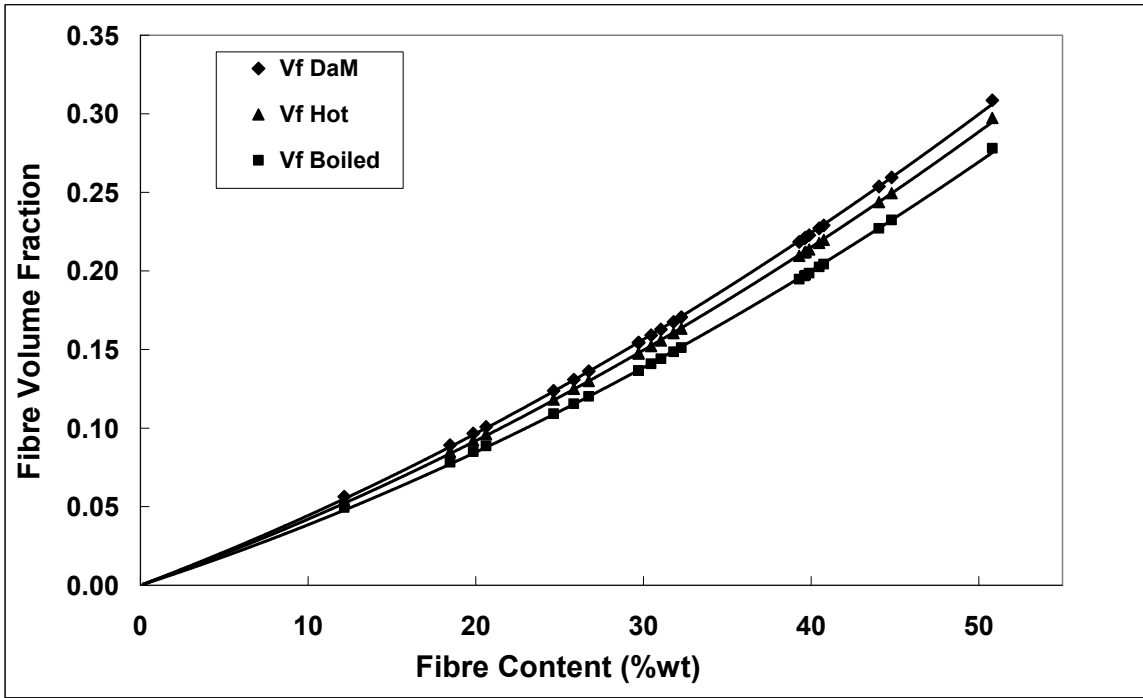


Figure 10 Fibre volume fraction versus weight fraction

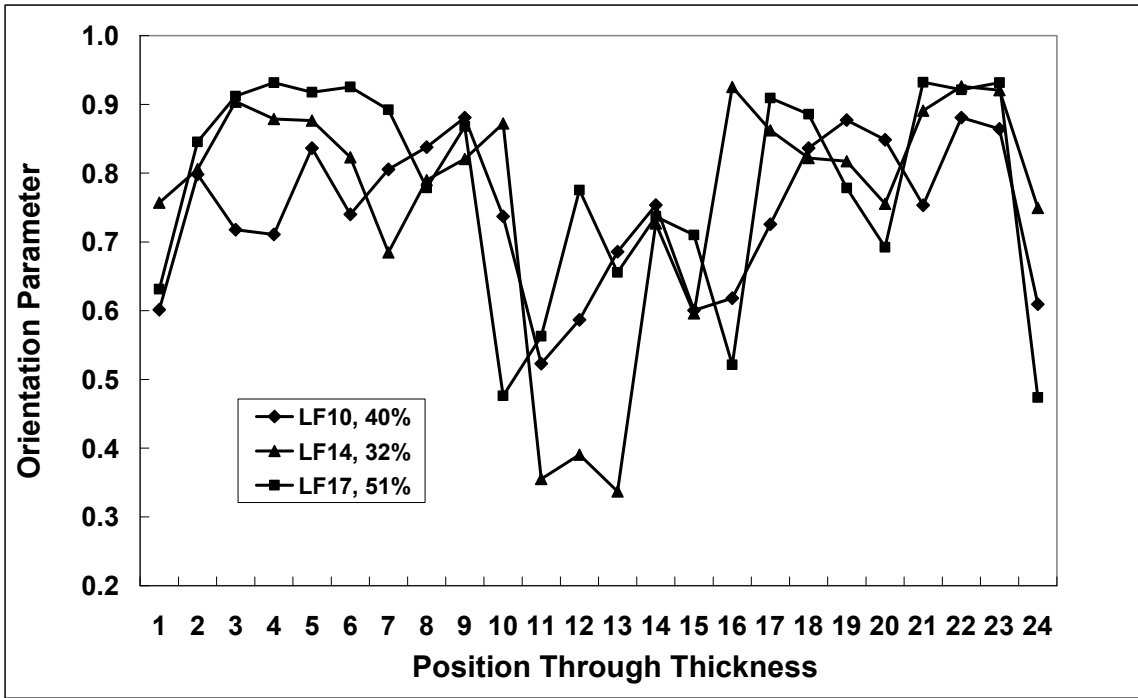


Figure 11 Fibre orientation parameter across sample thickness

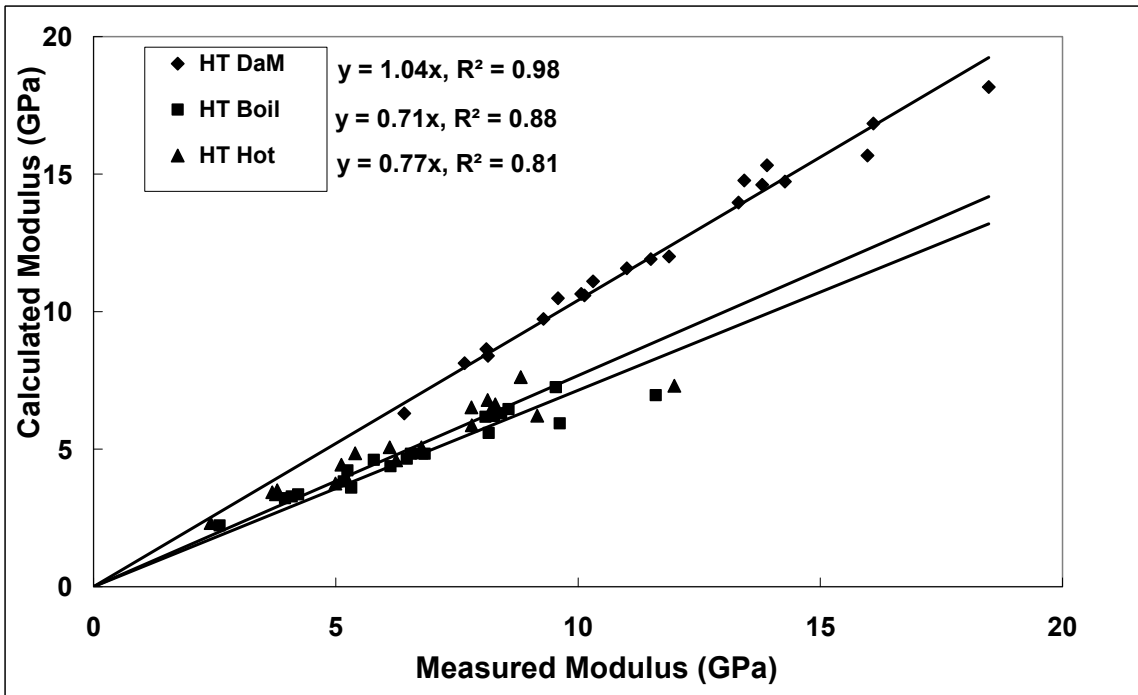


Figure 12 Comparison of Halpin-Tsai model predictions against experimental values

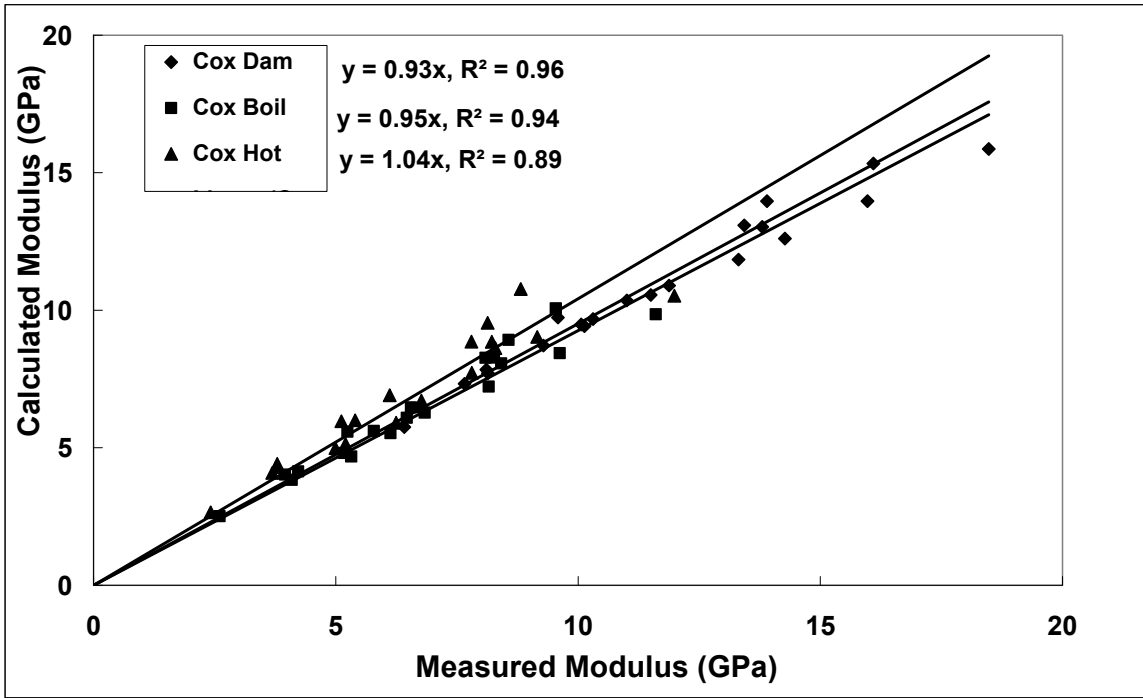


Figure 13 Comparison of Cox-Krenchel model predictions against experimental values

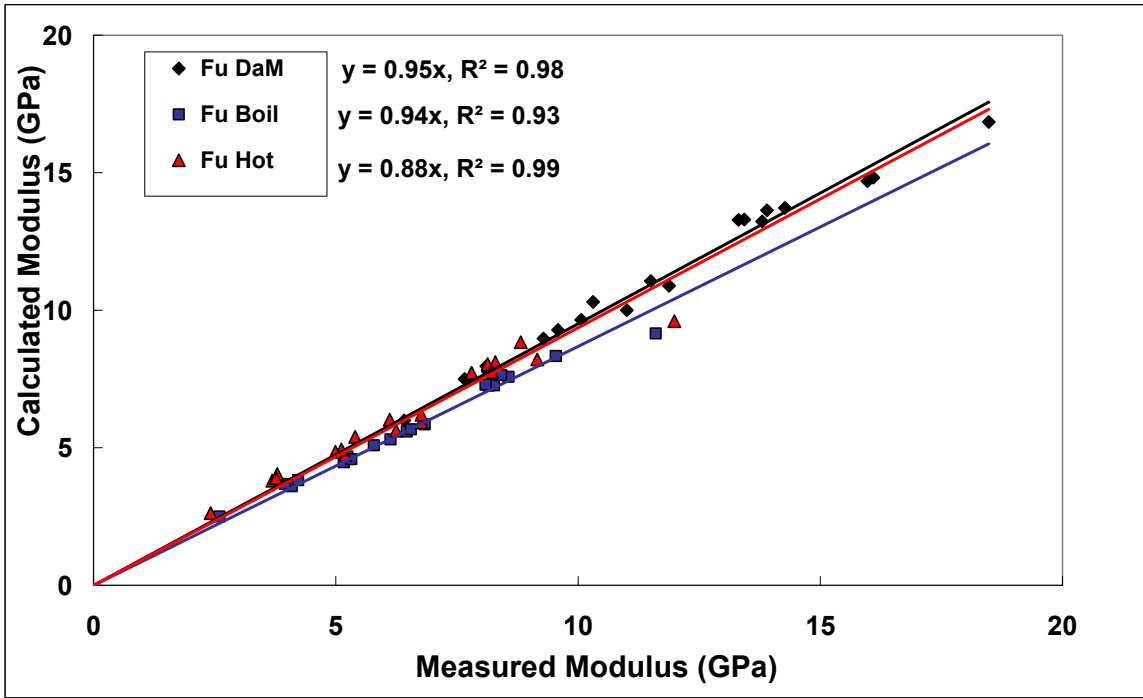


Figure 14 Comparison of Fu-Lauke model predictions against experimental values